

Final report
on key comparison Euramet.M.P-K15.1
in the pressure range from $3 \cdot 10^{-4}$ Pa to 1 Pa

Karl Jousten¹, Thomas Bock¹, Alper Elkatmis², Rifat Kangi², Suwat Phanakulwijit³, Janez Setina⁴

September 2020

Abstract

In the present comparison, the degrees of equivalence of the measurement standards for vacuum pressures from $3 \cdot 10^{-4}$ Pa up to 1 Pa of three NMIs were evaluated by comparison with the measurement standards PTB serving as linking laboratory to the two key comparisons CCM.P-K15 and CCM.P-K4. The three NMIs were IMT, Slovenia, NIMT, Thailand and TUBITAK-UME, Turkey. Two spinning rotor gauges served as transfer standards and showed a very good stability. All NMIs and at all pressures showed equivalence with the key comparison reference values of CCM.P-K15 and CCM.P-K4. Another NMI, CEM, Spain, took part in the comparison, but did not deliver any data.

¹ Physikalisch-Technische Bundesanstalt (PTB), Abbestr. 2-12, 10587 Berlin, Germany

² TUBITAK UME, TUBITAK Gebze Yerleskesi, P.K. 54, 41470 Gebze/KOCAELI, Turkey

³ National Institute of Metrology (Thailand), 3/4-5 Moo 3, klong 5, Klong Luang, Pathumthani 12120, Thailand

⁴ Institute of Metals and Technology (IMT), Lepi Pot 11, 1000 Ljubljana, Slovenia

1. Introduction

Three EURAMET members, CEM (Spain), MIRS-IMT(Slovenia), and TUBITAK-UME (Turkey) indicated their interest to link to the reference values of pressure from $3 \cdot 10^{-4}$ Pa to 1 Pa of CCM.P-K15 and CCM.P-K4 at 1 Pa to confirm their calibration and measurement capabilities (CMCs) in this range. In addition, the National Institute of Metrology Thailand (NIMT), wants to apply for CMC entries in this range and needs a linking comparison to confirm its measurement competence in this pressure range. To this end, the NIMT was included in this comparison.

Since PTB took part in both CCM.P-K15 and CCM.P-K4, PTB was chosen as linking and pilot laboratory.

As in the previous CCM [1] and EURAMET [2] comparisons in this pressure range, two spinning rotor gauges were chosen as transfer standards, which were to be calibrated at the following target pressures (nitrogen gas): $3 \cdot 10^{-4}$ Pa, $9 \cdot 10^{-4}$ Pa, $3 \cdot 10^{-3}$ Pa, $9 \cdot 10^{-3}$ Pa, $3 \cdot 10^{-2}$ Pa, $9 \cdot 10^{-2}$ Pa, 0.3 Pa, and 1 Pa.

2. Participating laboratories and their standards

Table 1 lists the laboratories that participated in this comparison in alphabetic order. One laboratory, Centro Espanol de Metrologia (CEM), Spain, did participate in the comparison, but did not deliver any calibration results to the pilot laboratory and was therefore deleted from the list.

In the second column of Table 1, the standards used for the calibration of the transfer standards are listed, in the third column it is characterised according to whether the standard is considered as primary or secondary, in the next column the traceability of the standard is given, the fifth column indicates, if the laboratory was listed in the CMC tables of the BIPM in the relevant pressure range at the time of the comparison.

Table 1 List of participants in alphabetic order and the standards used for the calibration of the transfer standards. CEM, Spain, participated, but did not deliver results.

Laboratory	Standard	Character of standard	Traceable to:	CMC listed
Institute of Metals and Technology (IMT), Slovenia	Static expansion system and spinning rotor gauge	Primary and Secondary	independent	yes
National Institute of Metrology Thailand (NIMT)	Spinning rotor gauge	Secondary	PTB	no
Physikalisch-Technische Bundesanstalt (PTB), Germany	Static expansion system	Primary	independent	yes
TUBITAK - Ulusal Metroloji Enstitusu (UME), Turkey	Static expansion system	Primary	independent	yes

Two types of standards were involved in the comparison: Static expansion systems as primary standards and spinning rotor gauges (SRG) as reference or secondary standards. IMT used both types of standards and was able to calibrate the secondary standard in its own facility and can therefore be considered as independent.

2.1. Calibration system at the IMT

Before taking part in this comparison IMT has developed a new static expansion system (Figure 1). The volumes are made of stainless steel AISI 304 and the whole system is of bakeable all-metal construction with metal seals.

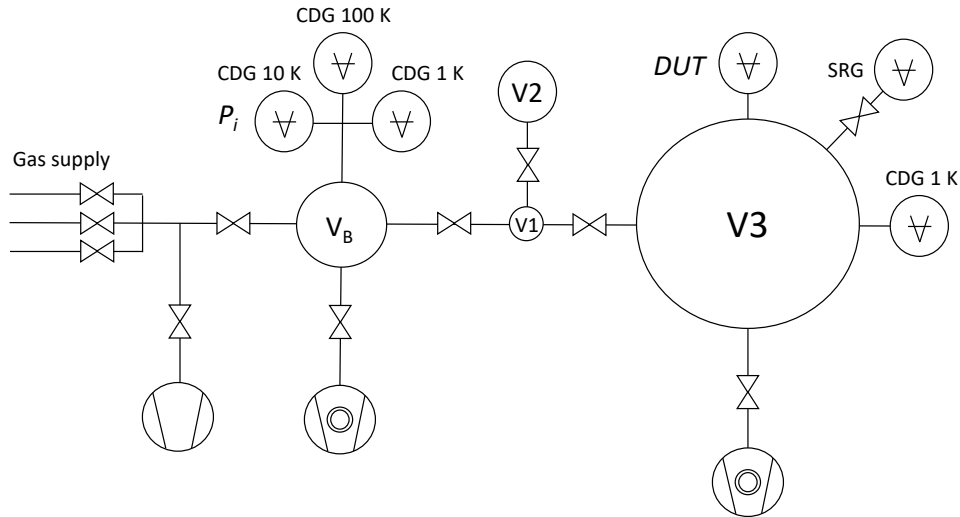


Figure 1 Scheme of static expansion system at IMT (DUT: Device under test, SRG spinning rotor gauge, CDG capacitance diaphragm gauge)

Two small volumes $V1$ (0.00506 L) and $V2$ (0.2470 L) serve as starting volumes for the expansion, which are interconnected by a valve. Gas may be expanded into the large chamber $V3$ (37.40 L) either from the smallest volume $V1$, or from a combination of the two volumes ($V1+V2$). Therefore, two volume ratios are available:

$$R_1 = \frac{V1 + V3}{V1} = 7392.4 \quad (1)$$

$$R_2 = \frac{V1 + V2 + V3}{V1 + V2} = 149.37 \quad (2)$$

Calibration gas is introduced from pure gas cylinders into ballast volume V_B (2.26 L) where three capacitance diaphragm gauges (CDGs) are connected for measurement of initial gas pressure before expansion. Gas from V_B is used to fill initial volumes $V1$ and $V2$.

IMT system is a fully independent primary vacuum system, where the two CDGs for measurement of initial pressure, CDG 10 K (full scale 10.0 kPa) in CDG 100 K (109 kPa), are directly traceable to a pressure balance Ruska 2465A in a range from 1.5 kPa to 109 kPa, which is further traceable to primary standards at PTB, Germany. The third CDG for initial pressure measurement (CDG 1K, full scale 1.09

kPa) is calibrated *in-situ* on the system by direct comparison with another CDG of the same FS range, mounted to V3. This reference CDG is calibrated by static expansion method using volume ratio R_2 .

At initial gas pressure 75 Pa (7% of FS range of CDG 1K), and using volume ratio $R_1=7392$, the system enables generation of calibration pressure 0.01 Pa in a single expansion. This is the lowest pressure point, which is usually generated by static expansion method in IMT system. For calibrations below 0.01 Pa a direct comparison method with a reference gauge is applied. To this end, a spinning rotor gauge (SRG) is permanently attached to the large expansion chamber V3. This reference SRG is calibrated *in-situ* by the static expansion method in a pressure range from 0.1 Pa to 1 Pa in steps 0.1 Pa. Intercept of linear regression line through data points gives the effective momentum accommodation coefficient of SRG rotor in molecular regime $\sigma(p \rightarrow 0)$. The main uncertainties are given in the following Table 2.

Table 2 Main uncertainty components for IMT primary static expansion system at the time of this comparison. All uncertainties are given as standard uncertainty with a coverage factor $k=1$. Not all uncertainties apply at the same time.

		nominal value	uncertainty ($k=1$)	relative uncertainty ($k=1$)
Pressure ratio	R_1	7400	3	0.041%
initial gas pressure	p_1 / kPa	1.5 to 109		0.050%
	p_1 / kPa	< 1.5		0.065%
temperature of large volume	T_{V1} / K	300	0.12	0.040%
temperature of small volume	T_{V3} / K	300	0.06	0.020%
gas pressure after expansion	p_2 / Pa	0.2 to 15		0.078%
	p_2 / Pa	0.01 to 0.2		0.089%
SRG	σ	1	0.0009	0.09%
	offset / Pa		3.5×10^{-7}	
SRG reference pressure	P / Pa	1×10^{-5} to 0.1	$\sqrt{(0.09\%)^2 + (3.5 \times 10^{-7} \text{ Pa})/P}$	

2.2. National measurement standard of NIMT

The calibration system model CS1002 from the Leybold company was used for the calibration of the transfer standards. The calibration chamber (cylindrical shape domed ends) is designed according to the international standard ISO 3567. Its volume is approximately 20 L. The chamber has eight CF35 ports on the same equatorial plane to connect the vacuum gauges. As reference gauges are available one spinning rotor gauge (SRG), one hot cathode ion gauge and three capacitance diaphragm gauges

(CDGs), all traceable to PTB. A turbomolecular pump, which was connected in series with a rotary pump (with oil trap), was used to evacuate the system. During the calibration, the pressure inside the calibration chamber was set between $3 \cdot 10^{-4}$ Pa to 1 Pa using a stationary equilibrium method. The SRG was used as a reference gauge in this comparison. The transfer standards and the reference SRG were connected in the same horizontal plane, perpendicular to the cylindrical axis of symmetry. The gas inlet during the calibration was in the tubing between the calibration chamber and pumping system.

2.3. Static expansion systems of the PTB (linking and pilot laboratory)

Two primary standards of the PTB, named SE1 and SE2, both realizing pressures using the static expansion method, were involved in the comparison.

In SE1 pressures are generated by expanding gas of known pressure from a very small volume V_4 of 17 mL directly into a volume of 233 L, or by two successive expansions from a volume $V_1 = 17$ mL into an intermediate volume of 21 L including V_4 and then from V_4 into the 233 L vessel. The regular operational range of SE1 is 10^{-6} Pa up to 1 Pa. The system is described in more detail in references [3] and [4]. This standard served as link to CCM.P-K15.

The system, called SE2 [4]- [6], served as an additional link to CCM.P-K4, which was performed for a pressure range from 1 Pa to 1 kPa. SE2 was one of the primary standards compared in CCM.P-K4.

The target pressures from 0.09 Pa to 1 Pa were measured both with SE1 and SE2, which agreed within their combined uncertainties. In order to avoid leaps between the standards taken at different times, the values of σ (see Eq. (3)) of SE1 were modified by scaling factors of 0.9994, 1.0010 and 0.9983 for the three measurements at PTB, respectively, for Rotor 1, and 0.9993, 1.0014 and 0.9984 for Rotor 2.

2.4. Static expansion system of the UME

The multi-stage static expansion system MSSE1 has been used for generating the calibration pressures [7]. The whole apparatus is UHV compatible and consists of 6 vessels. In operation, a sample of gas is trapped in one of the small vessels and then expanded into the next large and small vessels, which have previously been evacuated to a low pressure. This procedure was then repeated using the subsequent expansion steps until the gas expands in the calibration vessel. To generate the target pressures of $3 \cdot 10^{-4}$ Pa and $9 \cdot 10^{-4}$ Pa, the gas was expanded twice in the first stage. The initial gas pressure was measured using a calibrated quartz Bourdon tube gauge. The system is described in more detail in [7].

3. Transfer standards

Two spinning rotor gauges (SRG) have been chosen for the comparison. The SRG [8] is widely accepted as a transfer standard [9], [10] due to its measurement accuracy and long-term and transport stability.

Two devices were used in order to further reduce the influence of transport-instabilities, to produce redundancy, and to increase the accuracy of the comparison.

Only one controller provided by UME was circulated, because the participating laboratories had a spare controller available, so that the two transfer gauges could be calibrated at the same time on the same standard. The exception was NIMT who had to calibrate the SRGs separately on different days.

PTB used two spinning rotor gauges with known long and stable calibration history from their stock (Table 3). Both rotors (Rotor 1 and Rotor 2) were etched stainless steel balls, with a nominal diameter of 4.762 mm, embedded in a 8 mm OD tube (“finger”) with a DN16 CF flange.

Table 3 Transfer standards used for the comparison

Transfer standard	Rotor 1	Rotor 2
Internal no	9	12
Material	Etched stainless steel	Etched stainless steel
Nominal diameter	4.762 mm	4.762 mm
Nominal density	$7.715 \cdot 10^3 \text{ kg/m}^3$	$7.715 \cdot 10^3 \text{ kg/m}^3$

Each finger was sealed with a special all metal valve [11], which had two functions: 1. To seal the rotor in the finger so that it could be transported under vacuum. 2. To fix the rotor during transportation so that the surface would not be changed due to milling and friction effects of the rolling ball.

Transport under vacuum required that the valve was only opened when it was connected to high vacuum and, before transportation, the valve was closed under high vacuum conditions. To ensure free spinning of the rotor the valve had to be completely opened.

4. Calibration constant

The value to be calibrated by each laboratory j for each pressure for each rotor i was the effective accommodation factor σ_{ij} [8], often called σ_{eff} , which is mainly determined by the tangential momentum accommodation factor of the gas molecules to the rotor, and partly by the energy accommodation factor [8] and additionally by using nominal values for diameter and density of the rotors instead of the real ones.

σ_{ij} was determined by the following equation:

$$\sigma_{ij} = \sqrt{\frac{8kT_j}{\pi m}} \cdot \frac{\pi d_i \rho_i}{20p_j} \left(\left(\frac{\dot{\omega}}{\omega} \right)_i - RD_i(\omega) \right) \quad (3)$$

Herein p_j is the generated pressure of nitrogen gas in the standard, T_j the temperature of gas in the calibration chamber, d_i and ρ_i are the (nominal) diameter and density of the rotor i , m is the molecular mass of nitrogen, $(\dot{\omega}/\omega)$, also called DCR, is the relative deceleration rate of the rotor frequency ω ,

and RD is a pressure independent residual drag, caused by eddy current losses in the surrounding metal structures and the rotor itself.

The determination of $RD(\omega)$ was considered as part of the calibration, because it affects its accuracy, and was the responsibility of each laboratory. Proposals how to perform it were given in the protocol.

It is well known [8] that in the molecular regime up to about $3 \cdot 10^{-2}$ Pa σ_{eff} is pressure independent. For this reason, it was clear, a priori, that any significant pressure dependencies are likely to be due to measurement errors or problems of the calibration standard.

The temperatures of the measurement systems were monitored. The mean temperature during all calibrations was 296.0K with the lowest value at 295.4 K and the highest at 297.2 K. Since the temperature dependence of the accommodation factor is only in the $10^{-4}/\text{K}$ range [12], this dependence could be neglected in the evaluation of the results.

5. Organisation of the comparison and chronology

In order to reduce the effects of long-term and transport instabilities of the rotors, it was decided that after two or three participants the rotors were to be returned to the pilot laboratory for re-calibration. For the determination of the transport instability it was assumed that the primary standard of the pilot laboratory is stable which was confirmed by previous comparisons.

Table 4 presents the actual chronology of the calibrations including the calibrations at CEM that later did not deliver results.

Table 4 Chronology of measurements

Calibrating Laboratory	Date	Note
PTB 1	May 2017	
NIMT, Thailand	July 2017	Two SRGs not calibrated at the same time
UME, Turkey	November 2017	
PTB 2	March 2018	
IMT, Slovenia	June 2018	
CEM, Spain	November 2018	Faulty pump makes calibration impossible. Transfer standard had to be returned to PTB for expiration of ATA Carnet
CEM, Spain	November 2019	Measurements, but no results submitted
PTB 3	May 2020	

6. Calibration procedure and results to be reported

The following calibration procedure was agreed upon before the comparison: Each laboratory was to calibrate the two SRGs at the following 8 nominal target pressures p_t for nitrogen pressure in ascending order: $3 \cdot 10^{-4}$ Pa, $9 \cdot 10^{-4}$ Pa, $3 \cdot 10^{-3}$ Pa, $9 \cdot 10^{-3}$ Pa, $3 \cdot 10^{-2}$ Pa, $9 \cdot 10^{-2}$ Pa, 0.3 Pa, 1 Pa.

A tolerance of $\pm 10\%$ in hitting the nominal pressure was accepted for $p_t < 9 \cdot 10^{-2}$ Pa and $\pm 5\%$ for $9 \cdot 10^{-2}$ Pa, 0.3 Pa, 0.9 Pa. Each target pressure had to be generated 3 times. This meant that in static expansion and comparison systems, after a measurement at the target point, the system was pumped down to residual pressure conditions and the same point re-generated. In total $8 \cdot 3 = 24$ points were measured in this way and were considered as one calibration sequence. It was required that this calibration sequence be repeated at least once on another day.

The readings of each of the SRGs were to be sampled in the following manner:

- 5 repeat points at 30 s or 20 s intervals for the target points $3 \cdot 10^{-4}$ Pa, $9 \cdot 10^{-4}$ Pa, and $3 \cdot 10^{-3}$ Pa.
- 3 repeat points at 30 s or 20 s intervals for $9 \cdot 10^{-3}$ Pa, $3 \cdot 10^{-2}$ Pa, $9 \cdot 10^{-2}$ Pa.
- 3 repeat points at 10 s or 20 s intervals for 0.3 Pa and 1 Pa.

It was agreed that no bake-out should be performed with the rotors.

Since σ_{eff} is pressure dependent for $p > 3 \cdot 10^{-2}$ Pa, which may make the comparison inaccurate, when the target pressures are not hit exactly, it was agreed that a linear fit line through the points $\sigma_{ij}(p_j \approx 9 \cdot 10^{-2}$ Pa), $\sigma_{ij}(p_j \approx 0.3$ Pa), and $\sigma_{ij}(p_j \approx 1$ Pa) would be used to calculate σ_{ij} at the exact target pressures in the following manner

$$\sigma_{ij} = (\sigma_{ij})_{\text{det}} + (p_t - p_j) \cdot m_i \quad (4)$$

p_t are the nominal target pressures 0.09 Pa, 0.3 Pa, 1 Pa, p_{stj} the generated pressures close to p_t , $(\sigma_{ij})_{\text{det}}$ the values determined by the calibration at p_j , and m_i the slope of the fit line for rotor i . The uncertainty of the m_i will be neglected in the following since the p_j were very close to the p_t .

At the end of this calibration procedure, for each generated p_{stj} near the respective target point and for each rotor i and for each of the calibration sequences (2 or 3) a value for σ_{ij} existed and was reported to the pilot laboratory. With the value of σ_{ij} each laboratory j reported the standard uncertainty $u(p_j)$ of p_j .

7. Uncertainties of reference standards and other systematic uncertainties

Eq. (3) can be rewritten by using the rotor related constant

$$K_i = \sqrt{\frac{8k \cdot 296.15 \text{ K}}{\pi m}} \cdot \frac{\pi d_i \rho_i}{20} \quad (5)$$

and

$$DCR_i = \left(\frac{\dot{\omega}}{\omega} \right)_i \quad (6)$$

to

$$\sigma_{ij} = \sqrt{\frac{T_j}{296.15 \text{ K}}} \cdot \frac{K_i}{p_j} (DCR_i - RD_i(\omega)). \quad (7)$$

The K_i value was the same for each laboratory and can be considered as a constant, so that for the systematic (Type B) uncertainty of σ_{ij} the contributions of T_j , p_j and RD have to be considered. Depending on the way of measurement, RD may have a systematic effect, when it is measured before and after a measurement series, or before and after the measurements of three target points. DCR_i is measured every time and has no systematic uncertainty common to each measured point. The variance of σ_{ij} due to Type B uncertainties is given by

$$u_B^2(\sigma_{ij}) = \left(\frac{\partial \sigma_{ij}}{\partial T_j}\right)^2 u_{T_j}^2 + \left(\frac{\partial \sigma_{ij}}{\partial RD_i}\right)^2 u_{RD_i}^2 + \left(\frac{\partial \sigma_{ij}}{\partial p_j}\right)^2 u_{p_j}^2. \quad (8)$$

The sensitivity factors are given by the following equations:

$$\frac{\partial \sigma_{ij}}{\partial T_j} = \frac{1}{2} \frac{K_i}{p_j} \frac{1}{\sqrt{296.15 T_j}} (DCR_i - RD_i) \quad T_j \text{ in K} \quad (9)$$

$$\frac{\partial \sigma_{ij}}{\partial RD_i} = - \frac{K_i}{p_j} \sqrt{\frac{T_j}{296.15}} \quad T_j \text{ in K} \quad (10)$$

$$\frac{\partial \sigma_{ij}}{\partial p_j} = - \frac{K_i}{p_j^2} \sqrt{\frac{T_j}{296.15}} (DCR_i - RD_i) \quad T_j \text{ in K} \quad (11)$$

Table 5 presents the relative standard uncertainties due to Type B uncertainties for the various standards. Type A uncertainties will show up in the scatter of data at repeat measurements.

Table 5 Relative standard uncertainties $u(p_j)$ of the reference pressures p_j at the target pressures p_i in the standard j as reported by the participants.

p_i in Pa	IMT	NIMT	PTB	UME
$3 \cdot 10^{-4}$	$1.5 \cdot 10^{-3}$	$1.4 \cdot 10^{-2}$	$3.2 \cdot 10^{-3}$	$2.7 \cdot 10^{-3}$
$9 \cdot 10^{-4}$	$9.8 \cdot 10^{-4}$	$5.7 \cdot 10^{-3}$	$3.2 \cdot 10^{-3}$	$2.7 \cdot 10^{-3}$
$3 \cdot 10^{-3}$	$9.1 \cdot 10^{-4}$	$5.4 \cdot 10^{-3}$	$3.2 \cdot 10^{-3}$	$2.2 \cdot 10^{-3}$
$9 \cdot 10^{-3}$	$9.0 \cdot 10^{-4}$	$3.7 \cdot 10^{-3}$	$3.2 \cdot 10^{-3}$	$2.1 \cdot 10^{-3}$
$3 \cdot 10^{-2}$	$9.0 \cdot 10^{-4}$	$4.9 \cdot 10^{-3}$	$3.2 \cdot 10^{-3}$	$2.1 \cdot 10^{-3}$
$9 \cdot 10^{-2}$	$9.0 \cdot 10^{-4}$	$3.7 \cdot 10^{-3}$	$1.0 \cdot 10^{-3}$	$2.1 \cdot 10^{-3}$
0.3	$8.0 \cdot 10^{-4}$	$3.4 \cdot 10^{-3}$	$9.2 \cdot 10^{-4}$	$1.6 \cdot 10^{-3}$
1	$8.0 \cdot 10^{-4}$	$3.7 \cdot 10^{-3}$	$8.6 \cdot 10^{-4}$	$1.6 \cdot 10^{-3}$

8. Reported results of each laboratory

For those laboratories which carried out 2 or 3 calibration sequences it was necessary to check if significant changes could be observed between the σ_{ij} for the different sequences. No such changes occurred in any of the laboratories. The mean value of all data for a single rotor and single target pressure could be taken for data reduction:

$$\sigma_{ij} = \frac{1}{n} \sum_{k=1}^n \sigma_{ijk} \quad n = 3, 6 \text{ or } 9 \quad (12)$$

The Type A uncertainties u_A were determined from

$$u_A^2(\sigma_{ij}) = \frac{n-1}{n-3} s_{\sigma_{ij}}^2, \quad (13)$$

where the ratio on the right hand side considers that only a relatively small number of measurements was taken [13] and $s_{\sigma_{ij}}^2$ is the square of the standard deviation of the mean of the repeat measurements σ_{ijk} . In the case of NIMT, only three measurements (at different days) were taken for each target pressure, which makes the application of Eq. (13) not possible. Instead we applied

$$u_A^2(\sigma_{ij}) = 1,32 \cdot \frac{1}{3} \sum_{k=1}^3 (\sigma_{ijk} - \overline{\sigma_{ij}})^2, \quad (14)$$

where the first factor on the righthand side considers that the degree of freedom is only 2.

The results reported by each laboratory and the corresponding uncertainties according to Eq. (8), (12), and (14) are shown in the following tables and figures.

Table 6 Accommodation factor (σ_1) measured by the laboratories for Rotor 1 and uncertainties calculated according to Eq. (8), (12), and (14)

p_t in Pa		PTB 1	NIMT	UME	PTB 2	IMT	PTB 3
3E-04	σ_1	1.0708	1.0641	1.0695	1.0772	1.0721	1.0732
	$u_A(\sigma_1)$	0.0018	0.0025	0.0003	0.0015	0.0004	0.0015
	$u_B(\sigma_1)$	0.0034	0.0156	0.0036	0.0034	0.0024	0.0034
9E-04	σ_1	1.0712	1.0636	1.0709	1.0741	1.0716	1.0721
	$u_A(\sigma_1)$	0.0029	0.0013	0.0018	0.0003	0.0001	0.0005
	$u_B(\sigma_1)$	0.0034	0.0072	0.0031	0.0034	0.0012	0.0034
3E-03	σ_1	1.0708	1.0641	1.0696	1.0746	1.0719	1.0713
	$u_A(\sigma_1)$	0.0002	0.0004	0.0001	0.0005	0.0002	0.0002
	$u_B(\sigma_1)$	0.0034	0.0070	0.0024	0.0034	0.0010	0.0034
9E-03	σ_1	1.0717	1.0656	1.0693	1.0761	1.0717	1.0717
	$u_A(\sigma_1)$	0.0002	0.0004	0.0000	0.0002	0.0001	0.0001
	$u_B(\sigma_1)$	0.0034	0.0053	0.0024	0.0034	0.0010	0.0035
3E-02	σ_1	1.0698	1.0633	1.0689	1.0742	1.0715	1.0699
	$u_A(\sigma_1)$	0.0001	0.0012	0.0000	0.0001	0.0002	0.0000
	$u_B(\sigma_1)$	0.0034	0.0065	0.0024	0.0034	0.0010	0.0034
9E-02	σ_1	1.0689	1.0635	1.0682	1.0733	1.0702	1.0692
	$u_A(\sigma_1)$	0.0000	0.0006	0.0002	0.0000	0.0001	0.0000
	$u_B(\sigma_1)$	0.0011	0.0048	0.0024	0.0011	0.0010	0.0011
3E-01	σ_1	1.0632	1.0595	1.0628	1.0677	1.0655	1.0636
	$u_A(\sigma_1)$	0.0000	0.0004	0.0000	0.0000	0.0001	0.0001
	$u_B(\sigma_1)$	0.0010	0.0049	0.0018	0.0010	0.0009	0.0010
1E+00	σ_1	1.0462	1.0444	1.0469	1.0509	1.0494	1.0464
	$u_A(\sigma_1)$	0.0001	0.0001	0.0000	0.0000	0.0002	0.0001
	$u_B(\sigma_1)$	0.0010	0.0047	0.0017	0.0010	0.0009	0.0010

Table 7 Accommodation factor (σ_2) measured by the laboratories for Rotor 2 and uncertainties calculated according to Eq. (8), (12), and (14)

p_t in Pa		PTB 1	NIMT	UME	PTB 2	IMT	PTB 3
3E-04	σ_2	1.1078	1.1058	1.1068	1.1109	1.1081	1.1049
	$u_A(\sigma_2)$	0.0018	0.0022	0.0006	0.0015	0.0004	0.0015
	$u_B(\sigma_2)$	0.0035	0.0148	0.0035	0.0035	0.0025	0.0035
9E-04	σ_2	1.1067	1.1078	1.1073	1.1102	1.1076	1.1034
	$u_A(\sigma_2)$	0.0029	0.0016	0.0017	0.0003	0.0002	0.0005
	$u_B(\sigma_2)$	0.0035	0.0067	0.0030	0.0035	0.0012	0.0035
3E-03	σ_2	1.1060	1.1061	1.1061	1.1099	1.1079	1.1032
	$u_A(\sigma_2)$	0.0002	0.0006	0.0001	0.0005	0.0002	0.0002
	$u_B(\sigma_2)$	0.0035	0.0064	0.0023	0.0035	0.0011	0.0035
9E-03	σ_2	1.1069	1.1066	1.1058	1.1119	1.1079	1.1035
	$u_A(\sigma_2)$	0.0002	0.0005	0.0000	0.0002	0.0001	0.0001
	$u_B(\sigma_2)$	0.0035	0.0051	0.0023	0.0035	0.0010	0.0036
3E-02	σ_2	1.1049	1.1058	1.1053	1.1099	1.1075	1.1016
	$u_A(\sigma_2)$	0.0001	0.0004	0.0000	0.0001	0.0002	0.0000
	$u_B(\sigma_2)$	0.0035	0.0060	0.0023	0.0035	0.0010	0.0035
9E-02	σ_2	1.1041	1.1041	1.1046	1.1090	1.1062	1.1009
	$u_A(\sigma_2)$	0.0000	0.0002	0.0002	0.0000	0.0001	0.0000
	$u_B(\sigma_2)$	0.0011	0.0052	0.0023	0.0011	0.0010	0.0011
3E-01	σ_2	1.0982	1.0994	1.0990	1.1031	1.1011	1.0952
	$u_A(\sigma_2)$	0.0000	0.0002	0.0000	0.0000	0.0001	0.0001
	$u_B(\sigma_2)$	0.0010	0.0050	0.0018	0.0010	0.0009	0.0010
1E+00	σ_2	1.0804	1.0830	1.0822	1.0853	1.0842	1.0773
	$u_A(\sigma_2)$	0.0001	0.0002	0.0000	0.0000	0.0001	0.0001
	$u_B(\sigma_2)$	0.0010	0.0049	0.0019	0.0010	0.0009	0.0010

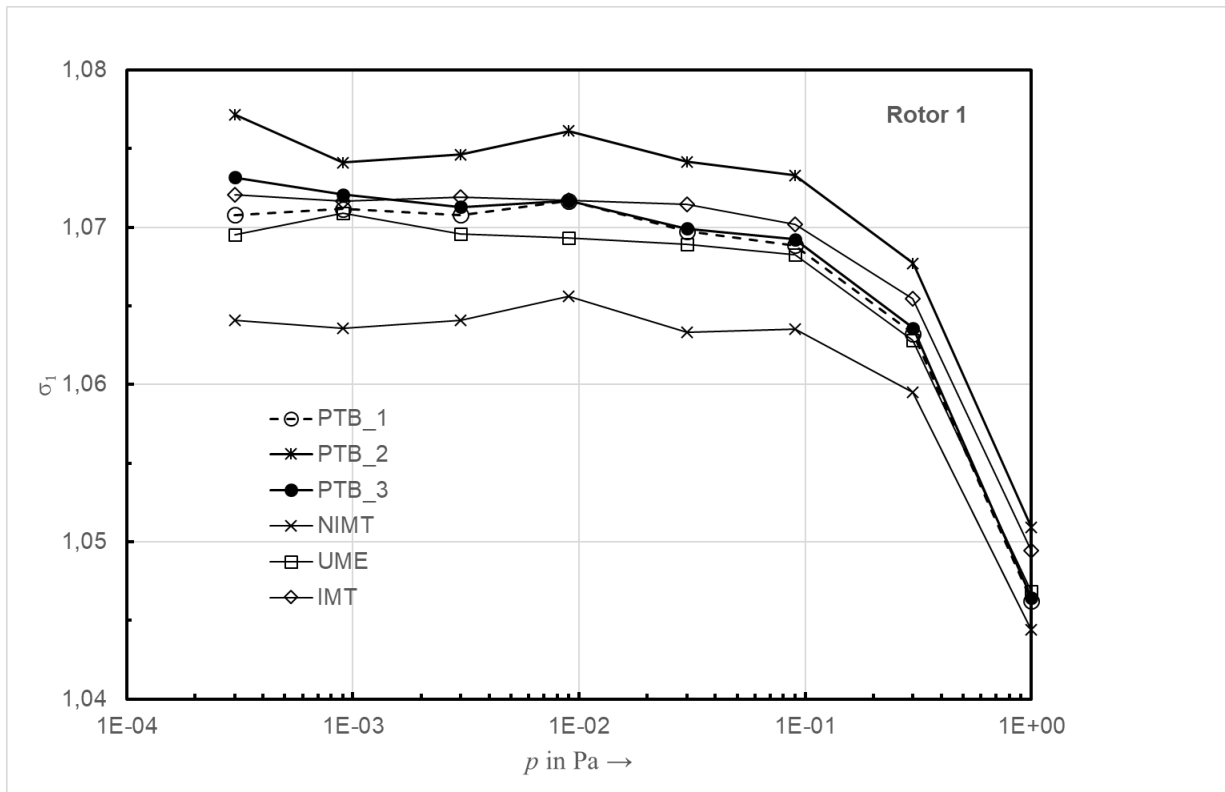


Figure 2 Accommodation factor (σ_1) measured by the laboratories for Rotor 1

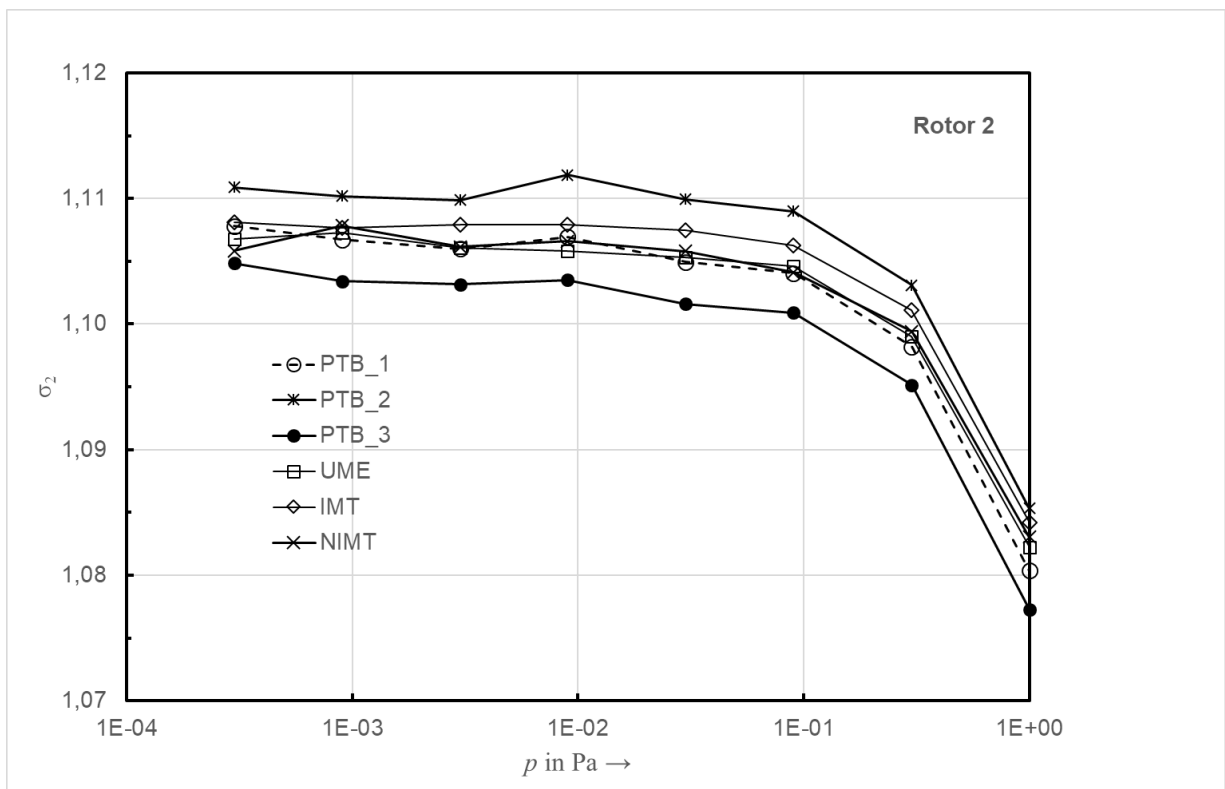


Figure 3 Accommodation factor (σ_2) measured by the laboratories for Rotor 2

It is well-known that the pressure independent σ -value in high vacuum (≤ 0.03 Pa) can be determined by measuring the pressure dependent σ -values between 0.09 Pa and 1 Pa and extrapolating them to zero

pressure [14]. During the comparison it was found that the PTB σ -values measured with the SE1 standard at pressures below 0.09 Pa slightly exceeded the extrapolated σ -value indicating a problem of the standard SE1. The difference was clearly and repeatably measurable, however, within the measurement uncertainties. It turned out that a loose throttle in the pneumatic system of the automatic valve caused the valve to close very quickly resulting in a positive differential pressure compared to the measured initial pressure before expansion. This effect is bigger in the molecular regime than in the viscous flow regime. The faulty throttle led to slightly higher σ -values (between 0.15% and 0.3%) below 0.09 Pa at PTB compared to the condition of the normally operating standard. For this reason, all σ -values below 0.09 Pa were multiplied with a factor of 0.998. The values of 0.09 Pa up to 1 Pa showed no systematic difference to values measured at the two other static expansion systems at PTB, SE2 and SE3. In this range the scaling factors mentioned at the end of Section 2.3 were applied.

9. Stability of transfer gauges

In order to monitor the stability of the calibration constant of the two rotors during the course of the comparison, the mean values of σ_1 and σ_2 between $9 \cdot 10^{-4}$ Pa and $3 \cdot 10^{-2}$ Pa of the pilot laboratory were calculated. Figure 4 shows the mean values, normalised to the first calibration of the comparison, PTB 1, to illustrate the relative changes. Table 8 shows the absolute values, which are, as discussed above, higher than the extrapolated values by about 0.17%.

Compared to the previous comparisons with similar standards [1], [2], the two SRGs showed a good stability within deviations of $\pm 0,4\%$ from the results at the start of the comparison. This enables us to use a single mean value for each rotor as reference for the pilot laboratory value, since the mean values of PTB 1 and PTB 2, and PTB 2 and PTB 3 are not significantly different. The long-term and transport instability was determined from the experimental standard deviation, again multiplied by 1.32 to consider a degree of freedom of 2.

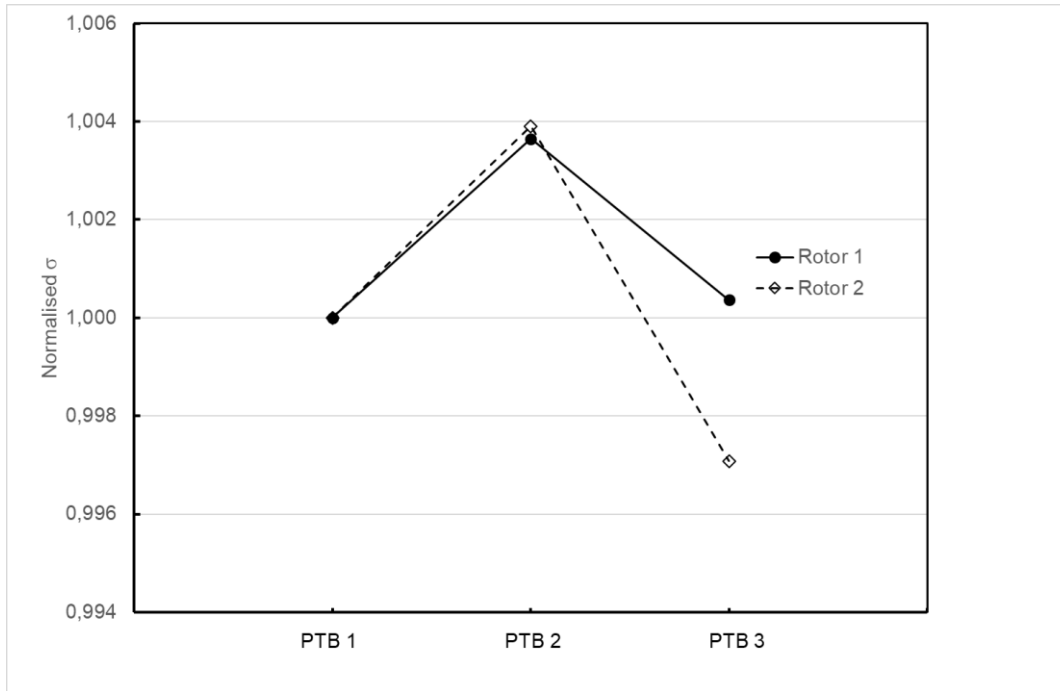


Figure 4 Normalised mean values in high vacuum of the pilot laboratory between $9 \cdot 10^{-4}$ Pa and $3 \cdot 10^{-2}$ Pa during the period of the comparison.

Table 8 Mean accommodation factors from $9 \cdot 10^{-4}$ Pa to $3 \cdot 10^{-2}$ Pa as measured by the pilot laboratory and the long-term and transport instability $u_{i,ts}$.

PTB#	σ_1	σ_2
PTB 1	1.0708	1.1061
PTB 2	1.0748	1.1105
PTB 3	1.0712	1.1029
mean $\sigma_{i,PTB}$	1.0723	1.1065
$u_{i,ts}$	0.0028	0.0050

10. Data reduction

Since PTB was the only laboratory that could serve as linking laboratory to the reference pressure values determined in CCM.P-K15 [1] and CCM.P-K4 [16], at first, a reference accommodation factor had to be determined for each target pressure p_t .

Since it is known that the accommodation factor is independent of pressure up to 30 mPa, we took the mean values of the three sequences at PTB in this range as shown in Table 8. For the target pressures $9 \cdot 10^{-2}$ Pa, 0,3 Pa and 1 Pa, we used the mean values accommodation factor of the three sequences at PTB shown in Table 9 and Table 10.

Table 9 Mean accommodation factors for 0,09 Pa, 0,3 Pa and 1 Pa for Rotor 1 as measured by the pilot laboratory

p_t in Pa	0.09	0.30	1.00
PTB1	1.0689	1.0632	1.0462
PTB2	1.0733	1.0677	1.0509
PTB3	1.0692	1.0636	1.0464
mean $\sigma_{1,PTB}$	1.0705	1.0648	1.0479

Table 10 Mean accommodation factors for 0,09 Pa, 0,3 Pa and 1 Pa for Rotor 2 as measured by the pilot laboratory

p_t in Pa	0.09	0.30	1.00
PTB1	1.1041	1.0982	1.0804
PTB2	1.1090	1.1031	1.0853
PTB3	1.1009	1.0952	1.0773
mean $\sigma_{2,PTB}$	1.1046	1.0988	1.0810

With these reference accommodation values it is possible to calculate for each participant (except the pilot laboratory) and for each SRG i a value of indicated pressure p_{ij} for a common hypothetical target pressure p_t by:

$$p_{ij} = p_t \cdot \frac{\sigma_{ij}}{\sigma_{iPTB}} \quad i = 1,2 \quad j = 1 \dots 3 \quad (15)$$

σ_{ij} denotes the mean accommodation factor according to Eq. (12) of SRG i for p_t as determined by laboratory j , σ_{iPTB} the reference accommodation values obtained at the pilot laboratory for p_t .

The p_{ij} in Eq. (15) are the predicted gauge readings, when the standards in the different laboratories realise the same value of target pressure p_t . The difference in the predicted gauge readings is taken as an indicator of the difference between true pressures actually realised or determined by the different standards. This latter difference between true pressures, when the standards are set to produce the same transfer gauge reading near the target pressure, is to a very good approximation (provided that the differences are small) equal to the difference in the predicted gauge readings but of opposite sign.

Since p_t is simply a nominal value without uncertainty, the uncertainty of p_{ij} is calculated from the following equation (except for the pilot laboratory):

$$u(p_{ij}) = p_{ij} \sqrt{\left(\frac{u_A(\sigma_{ij})}{\sigma_{ij}}\right)^2 + \left(\frac{u_B(\sigma_{ij})}{\sigma_{ij}}\right)^2 + \left(\frac{u_B(\sigma_{iPTB})}{\sigma_{iPTB}}\right)^2 + \left(\frac{u_{i,ls}}{\sigma_{iPTB}}\right)^2} \quad (16)$$

$u_A(\sigma_{ij})$ were given in Eqs. (13) and (14), $u_B(\sigma_{ij})$ and $u_B(\sigma_{iPTB})$ in Eq. (8), $u_{i,ls}$ in Table 8. $u_A(\sigma_{iPTB})$ is included in $u_{i,ls}$. We should note here that we neglect any correlation between the measurement standard of NIMT and the primary standard of PTB, although the first is traceable to the latter. The reason is that the systematic uncertainties at NIMT are much higher than the ones at PTB (see Section 7) and the

results of NIMT show that Rotor 1 and Rotor 2 gave quite different results compared to PTB, which indicates an at least insignificant correlation.

In the case of the pilot laboratory, the mean of all three sequences is taken:

$$p_{i,PTB} = p_t \cdot \frac{\sigma_{iPTB1} + \sigma_{iPTB2} + \sigma_{iPTB3}}{3 \cdot \sigma_{iPTB}} \quad i = 1,2 \quad (17)$$

In the molecular regime up to 30 mPa, since σ_{iPTB} is taken as mean between $9 \cdot 10^{-4}$ Pa and $3 \cdot 10^{-2}$ Pa, p_{iPTB} may be slightly different from p_t , in the transition regime ($> 3 \cdot 10^{-2}$ Pa), however, it will be identical to p_t .

The uncertainty is determined by

$$u(p_{i,PTB}) = p_{i,PTB} \sqrt{\frac{u_A^2(\sigma_{i,PTB1}) + u_A^2(\sigma_{i,PTB2}) + u_A^2(\sigma_{i,PTB3})}{(\sigma_{i,PTB1} + \sigma_{i,PTB2} + \sigma_{i,PTB3})^2} + \left(\frac{u_B(\sigma_{i,PTB})}{\sigma_{iPTB}}\right)^2 + \left(\frac{u_{i,lts}}{\sigma_{i,PTB}}\right)^2} \quad (18)$$

It needs to be noted that any systematic error of p_{PTB} common to all sequences cancel out in Eq. (17), but the realisation of p_t is uncertain due to the $u_B(p_{PTB})$. For this reason, this term is considered in Eq. (18).

Having done this, for each laboratory and for each target point there are two values: p_{1j} and p_{2j} . Generally, these values will be slightly different. By the weighted mean, which ensures that the SRG with the higher long-term stability and/or less scatter in the results gets more weight than the other, we calculate a single value for each participant:

$$\tilde{p}_j = \frac{\sum_{i=1}^2 \frac{p_{ij}}{u_A^2(p_{ij})}}{\sum_{i=1}^2 \frac{1}{u_A^2(p_{ij})}} \quad (19)$$

p_{1j} and p_{2j} are correlated, because the same standard j was used to determine σ_{1j} and σ_{2j} . It was shown in [2] that the easiest way to consider this correlation is to omit $u_B(p_j)$.

It is

$$u_A^2(p_{ij}) = p_{ij}^2 \left(\left(\frac{u_A(\sigma_{ij})}{\sigma_{ij}} \right)^2 + \left(\frac{u_{i,lts}}{\sigma_{iPTB}} \right)^2 \right). \quad (20)$$

The standard uncertainty of \tilde{p}_j is

$$u(\tilde{p}_j) = \sqrt{\left(\frac{u_B(p_j)}{p_j} \right)^2 \tilde{p}_j^2 + \left(\sum_{i=1}^2 \frac{1}{u_A^2(p_{ij})} \right)^{-1}} \quad (21)$$

The second term under the square root describes the influences, which are due to the rotor instability and scatter of data. The first term under the square root describes the influence of the uncertainty of the

pressure p_j generated by standard j that correlates to both p_{1j} and p_{2j} and the uncertainty of the realisation at PTB:

$$\left(\frac{u_B(p_j)}{p_j}\right)^2 = \left(0,5 \cdot \frac{u_B(\sigma_{1j})}{\sigma_{1j}} + 0,5 \cdot \frac{u_B(\sigma_{2j})}{\sigma_{2j}}\right)^2 + \left(0,5 \cdot \frac{u_B(\sigma_{1PTB})}{\sigma_{1PTB}} + 0,5 \cdot \frac{u_B(\sigma_{2PTB})}{\sigma_{2PTB}}\right)^2 \quad (22)$$

For the values of the ratios $u(\sigma_{1PTB})/\sigma_{1PTB}$ and $u(\sigma_{2PTB})/\sigma_{2PTB}$ it is sufficient to select one of the sequences PTB 1...3, since the ratios were practically identical for the different sequences.

With the mean value \tilde{p}_j one value with a corresponding standard uncertainty exists for each laboratory and for each target pressure.

The following tables give the results for p_{ij} (

Table 11 and Table 12) and \tilde{p}_j (Table 13).

Table 11 Values for p_{ij} according to Eq. (15) (for PTB Eq. (17)) and the associated uncertainty according to Eq. (16) (for PTB Eq. (18)) for each participant.

p_t in Pa		NIMT	UME	IMT	PTB
3E-04	p_{ij}	2.977E-04	2.992E-04	2.999E-04	3.004E-04
	$u(p_{1j})$	4.6E-06	1.6E-06	1.4E-06	1.5E-06
9E-04	p_{ij}	8.927E-04	8.988E-04	8.995E-04	9.001E-04
	$u(p_{1j})$	7.2E-06	4.8E-06	3.9E-06	4.5E-06
3E-03	p_{ij}	2.977E-03	2.992E-03	2.999E-03	3.000E-03
	$u(p_{1j})$	2.3E-05	1.4E-05	1.3E-05	1.3E-05
9E-03	p_{ij}	8.944E-03	8.975E-03	8.995E-03	9.007E-03
	$u(p_{1j})$	5.8E-05	4.2E-05	3.8E-05	3.8E-05
3E-02	p_{ij}	2.975E-02	2.991E-02	2.998E-02	2.997E-02
	$u(p_{1j})$	2.2E-04	1.4E-04	1.3E-04	1.2E-04
9E-02	p_{ij}	8.942E-02	8.981E-02	8.998E-02	9.000E-02
	$u(p_{1j})$	4.8E-04	3.2E-04	2.7E-04	2.6E-04
3E-01	p_{ij}	2.985E-01	2.994E-01	3.002E-01	3.000E-01
	$u(p_{1j})$	1.6E-03	9.9E-04	8.8E-04	8.5E-04
1E+00	p_{ij}	9.9669E-01	9.9906E-01	1.0015E+00	1.0000E+00
	$u(p_{1j})$	5.3E-03	3.3E-03	2.9E-03	2.9E-03

Table 12 Values for p_{2j} according to Eq. (15) (for PTB Eq. (17)) and the associated uncertainty according to Eq. (16) (for PTB Eq. (18))for each participant.

p_t in Pa		NIMT	UME	IMT	PTB
3E-04	p_{2j}	2.998E-04	3.001E-04	3.004E-04	3.004E-04
	$u(p_{2j})$	4.4E-06	1.9E-06	1.8E-06	1.8E-06
9E-04	p_{2j}	9.011E-04	9.006E-04	9.009E-04	9.002E-04
	$u(p_{2j})$	7.5E-06	5.7E-06	5.1E-06	5.5E-06
3E-03	p_{2j}	2.999E-03	2.999E-03	3.004E-03	3.000E-03
	$u(p_{2j})$	2.4E-05	1.8E-05	1.7E-05	1.7E-05
9E-03	p_{2j}	9.001E-03	8.994E-03	9.012E-03	9.008E-03
	$u(p_{2j})$	6.5E-05	5.3E-05	5.1E-05	5.0E-05
3E-02	p_{2j}	2.998E-02	2.997E-02	3.003E-02	2.997E-02
	$u(p_{2j})$	2.3E-04	1.8E-04	1.7E-04	1.7E-04
9E-02	p_{2j}	8.996E-02	9.000E-02	9.013E-02	9.000E-02
	$u(p_{2j})$	5.9E-04	4.6E-04	4.3E-04	4.2E-04
3E-01	p_{2j}	3.002E-01	3.001E-01	3.006E-01	3.000E-01
	$u(p_{2j})$	2.0E-03	1.5E-03	1.5E-03	1.4E-03
1E+00	p_{2j}	1.0019E+00	1.0012E+00	1.0030E+00	1.0000E+00
	$u(p_{2j})$	6.6E-03	5.1E-03	4.9E-03	4.7E-03

Table 13 Values for \tilde{p}_j according to Eq. (19) and the associated uncertainty according to Eq. (21) for each participant.

p_t in Pa		NIMT	UME	IMT	PTB
3E-04	p_j	2.984E-04	2.994E-04	3.001E-04	3.004E-04
	$u(p_j)$	4.4E-06	1.5E-06	1.4E-06	7.2E-07
9E-04	p_j	8.949E-04	8.994E-04	8.998E-04	9.002E-04
	$u(p_j)$	6.8E-06	4.5E-06	3.7E-06	2.2E-06
3E-03	p_j	2.983E-03	2.994E-03	3.000E-03	3.000E-03
	$u(p_j)$	2.2E-05	1.3E-05	1.2E-05	6.9E-06
9E-03	p_j	8.958E-03	8.980E-03	8.999E-03	9.007E-03
	$u(p_j)$	5.6E-05	4.0E-05	3.7E-05	2.1E-05
3E-02	p_j	2.982E-02	2.992E-02	2.999E-02	2.997E-02
	$u(p_j)$	2.1E-04	1.3E-04	1.2E-04	6.8E-05
9E-02	p_j	8.956E-02	8.986E-02	9.002E-02	9.000E-02
	$u(p_j)$	4.7E-04	3.0E-04	2.4E-04	2.1E-04
3E-01	p_j	2.989E-01	2.996E-01	3.003E-01	3.000E-01
	$u(p_j)$	1.6E-03	8.9E-04	7.8E-04	6.9E-04

1E+00	p_i	9.9801E-01	9.9959E-01	1.0019E+00	1.0000E+00
	$u(p_j)$	5.1E-03	3.0E-03	2.6E-03	2.3E-03

11. Link to key comparisons CCM.P-K15 and CCM.P-K4

Since PTB was the only laboratory that took part in CCM.P-K15 and CCM.P-K4, this laboratory had to serve as link to these two key comparisons. PTB used the same standards in all three comparisons for the respective target pressures, so that it can be assumed that the bias to the respective key comparison reference value is the same in this comparison as in the past in the two key comparisons. No significant changes of the PTB measurement standards were made. In CCM.P-K15, each key comparison reference value was identical to the target pressure, in CCM.P-K4, the reference value was 1,002 Pa. The difference to 1 Pa exact, however, is of no significance, since the PTB primary standard realises the pressures around 1 Pa in an identical manner. Table 14 shows the relative deviation d' of the predicted gauge readings \tilde{p}_{PTB} at PTB to the reference value as evaluated in CCM.P-K15 [1] and CCM.P-K4 [16]. We repeat that the relative difference of the predicted gauge reading to the reference is to a very good approximation equal to the difference of generated or measured pressure in the standard to the reference, but of opposite sign.

$$d' = \frac{\tilde{p}_{PTB}}{p_{KC,ref}} - 1 \quad (23)$$

Table 14 Relative deviation d' and its expanded ($k=2$) uncertainty $U(d')$ of the predicted gauge readings at PTB to the reference value of the related comparison

Target pressure/Pa →	$3 \cdot 10^{-4}$	$9 \cdot 10^{-4}$	$3 \cdot 10^{-3}$	$9 \cdot 10^{-3}$	$3 \cdot 10^{-2}$	$9 \cdot 10^{-2}$	0,3	1
d' (CCM.P-K15)	-0.0033	-0.0032	-0.0029	-0.0016	-0.0020	-0.0026	-0.0027	-0.0036
$U(d')$	0.0129	0.0100	0.0099	0.0095	0.0098	0.0061	0.0055	0.0059
d' (CCM.P-K4)								0.000
$U(d')$								0.014

For linking this comparison to the two CCM comparisons, for each target pressure, we determine the predicted gauge reading, which PTB would have determined, if its generated pressure would have been identical to the respective key comparison reference value. These pressures are given by

$$p_{KC,ref} = \frac{\tilde{p}_{PTB}}{d' + 1} \quad (24)$$

The uncertainty of $p_{KC,ref}$ is given by

$$u(p_{\text{KC,ref}}) = p_{\text{KC,ref}} \sqrt{\left(\frac{u(\tilde{p}_{\text{PTB}})}{\tilde{p}_{\text{PTB}}}\right)^2 + \left(\frac{u(d')}{(d'+1)}\right)^2} \quad (25)$$

Table 15 lists the values of $p_{\text{KC,ref}}$ and $u(p_{\text{KC,ref}})$. Note that in Table 13 expanded uncertainties uncertainties were given.

Table 15 Reference predicted gauge readings $p_{KC,ref}$ and their uncertainties $u(p_{KC,ref})$ to compare with the predicted gauge readings of the participants.

p_i in Pa		CCM.P-K15	CCM.P-K4
$3 \cdot 10^{-4}$	$p_{KC,ref}$	3.014E-04	
	$u(p_{KC,ref})$	2.1E-06	
$9 \cdot 10^{-4}$	$p_{KC,ref}$	9.031E-04	
	$u(p_{KC,ref})$	5.0E-06	
$3 \cdot 10^{-3}$	$p_{KC,ref}$	3.009E-03	
	$u(p_{KC,ref})$	1.6E-05	
$9 \cdot 10^{-3}$	$p_{KC,ref}$	9.022E-03	
	$u(p_{KC,ref})$	4.8E-05	
$3 \cdot 10^{-2}$	$p_{KC,ref}$	3.003E-02	
	$u(p_{KC,ref})$	1.6E-04	
$9 \cdot 10^{-2}$	$p_{KC,ref}$	9.023E-02	
	$u(p_{KC,ref})$	3.4E-04	
0,3	$p_{KC,ref}$	3.008E-01	
	$u(p_{KC,ref})$	1.1E-03	
1	$p_{KC,ref}$	1.004E+00	1.000E+00
	$u(p_{KC,ref})$	3.8E-03	7.4E-03

To test the equivalence of the participant values \tilde{p}_j with the key comparison reference values $p_{KC,ref}$, we determine the relative difference d_j

$$d_j = \frac{\tilde{p}_j}{p_{KC,ref}} - 1 \quad (26)$$

for each participant and each target pressure with the expanded uncertainty $U(k=2)$

$$U(d_j) = 2 \cdot \sqrt{\left(\frac{u(\tilde{p}_j)}{p_{KC,ref}}\right)^2 + \left(\frac{\tilde{p}_j}{p_{KC,ref}^2}\right)^2 u^2(p_{KC,ref})} \quad (27)$$

For $j = PTB$, the first term under the square root is obsolete, since it is already considered in the uncertainty of $p_{KC,ref}$. Table 16 and

Table 17 show the results for d_j and the expanded uncertainties according to Eqs. (26) and (27).

Table 16 The relative differences d_j of predicted gauge readings of the participants to the predicted gauge readings, if PTB would have generated a pressure identical to the reference value of the comparison CCM.P-K15 (Eq. (26)). The expanded uncertainty is given by Eq. (27).

p_t in Pa		NIMT	UME	IMT	PTB
3E-04	d_j	-9.8E-03	-6.4E-03	-4.4E-03	-3.3E-03
	$U(d_j)$	3.2E-02	1.7E-02	1.6E-02	1.4E-02
9E-04	d_j	-9.0E-03	-4.1E-03	-3.6E-03	-3.2E-03
	$U(d_j)$	1.9E-02	1.5E-02	1.4E-02	1.1E-02
3E-03	d_j	-8.6E-03	-4.8E-03	-2.8E-03	-2.9E-03
	$U(d_j)$	1.8E-02	1.4E-02	1.4E-02	1.1E-02
9E-03	d_j	-7.0E-03	-4.6E-03	-2.5E-03	-1.6E-03
	$U(d_j)$	1.6E-02	1.4E-02	1.3E-02	1.1E-02
3E-02	d_j	-7.2E-03	-3.7E-03	-1.4E-03	-2.0E-03
	$U(d_j)$	1.8E-02	1.4E-02	1.3E-02	1.1E-02
9E-02	d_j	-7.5E-03	-4.1E-03	-2.4E-03	-2.6E-03
	$U(d_j)$	1.3E-02	1.0E-02	9.3E-03	7.6E-03
3E-01	d_j	-6.3E-03	-4.1E-03	-1.7E-03	-2.7E-03
	$U(d_j)$	1.3E-02	9.3E-03	8.8E-03	7.1E-03
1E+00	d_j	-5.6E-03	-4.0E-03	-1.7E-03	-3.6E-03
	$U(d_j)$	1.3E-02	9.6E-03	9.1E-03	7.5E-03

Table 17 The relative differences d_j of predicted gauge readings of the participants to the predicted gauge readings, if PTB would have generated a pressure identical to the reference value of the comparison CCM.P-K4 (Eq. (26)). The expanded uncertainty is given by Eq. (27).

p_t in Pa		NIMT	UME	IMT	PTB
1E+00	d_j	-2.0E-03	-4.1E-04	1.9E-03	0.0E+00
	$U(d_j)$	1.8E-02	1.6E-02	1.6E-02	1.5E-02

Clearly, due to our methodology the difference of the PTB values to the KC reference is the same as in the two key comparisons.

To easily see equivalence with the reference value or not, it is convenient to determine the so called E_n values, which are given by

$$E_n = \frac{d_j}{U(d_j)} \quad (28)$$

If $-1 \leq E_n \leq 1$, equivalence is assumed. The E_n values are shown in Table 18.

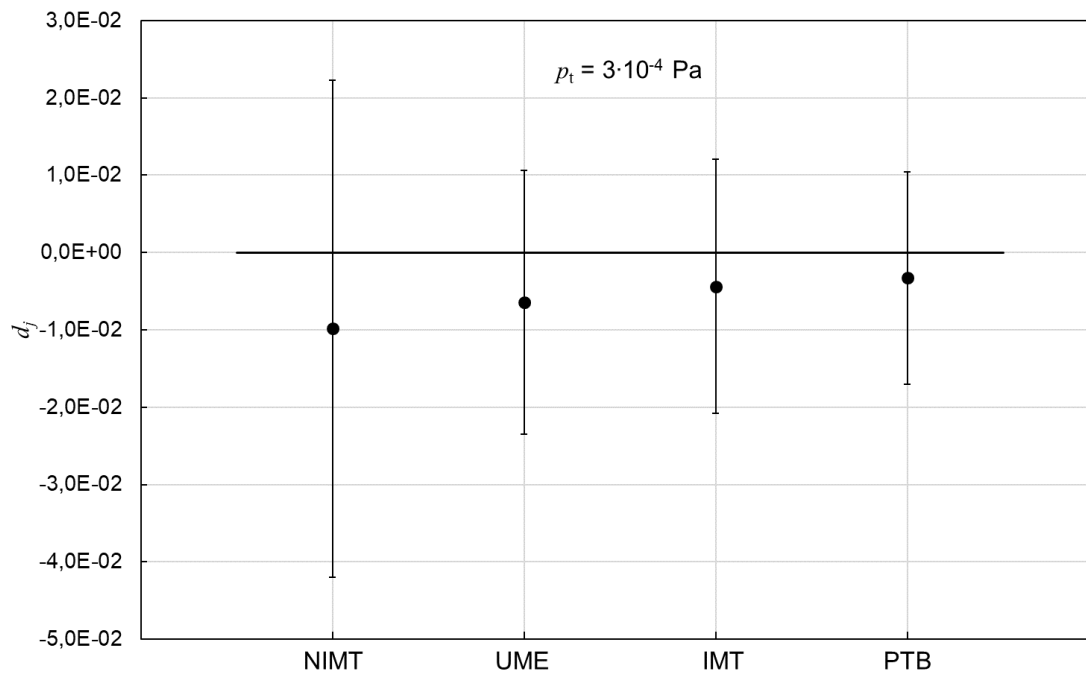
Table 18 The E_n values as defined in Eq. (28).

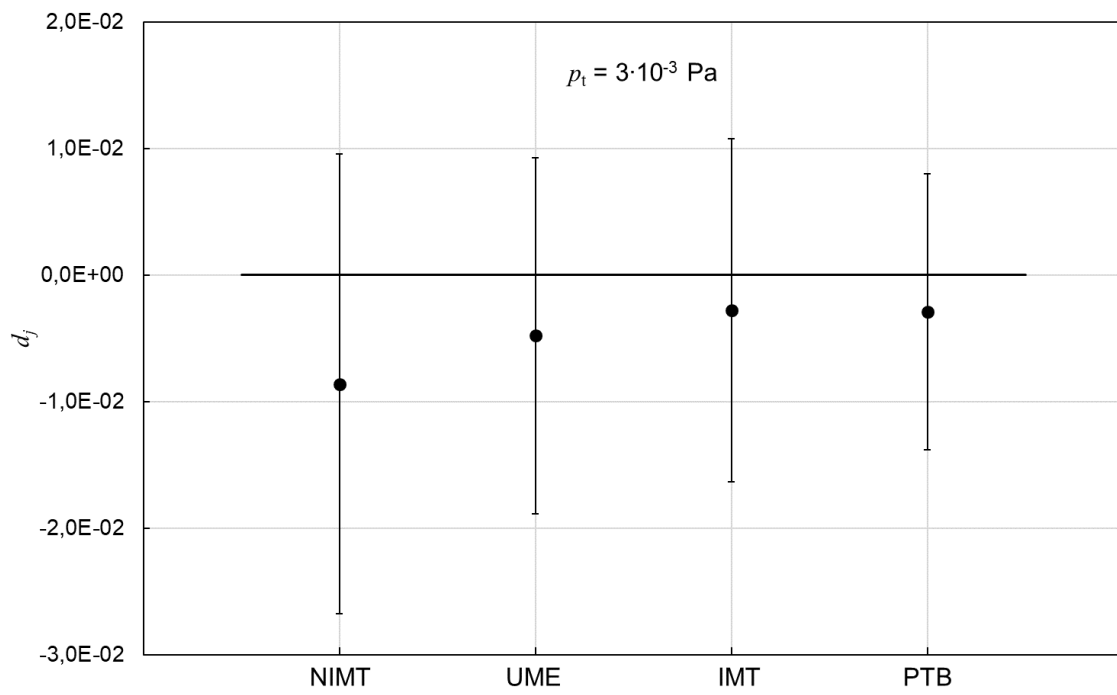
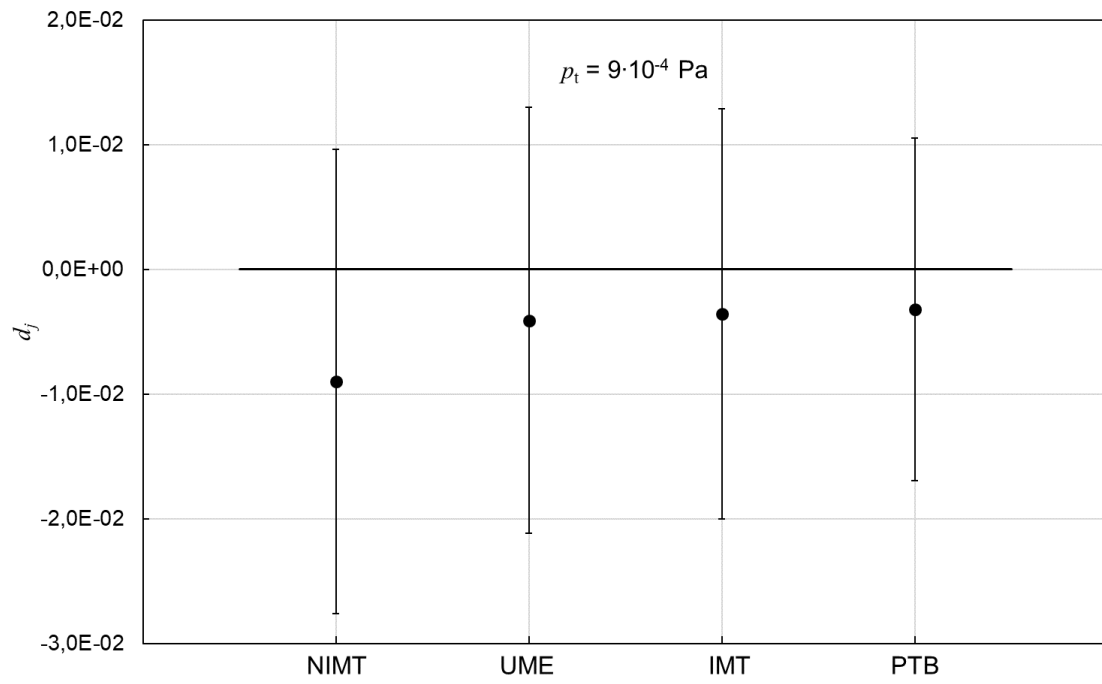
p_t in Pa	NIMT	UME	IMT	PTB
CCM.P-K15				
3E-04	-0.31	-0.38	-0.27	-0.24
9E-04	-0.48	-0.27	-0.26	-0.29
3E-03	-0.47	-0.34	-0.20	-0.27
9E-03	-0.44	-0.33	-0.19	-0.15
3E-02	-0.41	-0.26	-0.10	-0.19
9E-02	-0.58	-0.41	-0.26	-0.34
3E-01	-0.50	-0.44	-0.20	-0.38
1E+00	-0.44	-0.42	-0.19	-0.48
CCM.P-K4				
1E+00	-0.11	-0.03	0.12	0.00

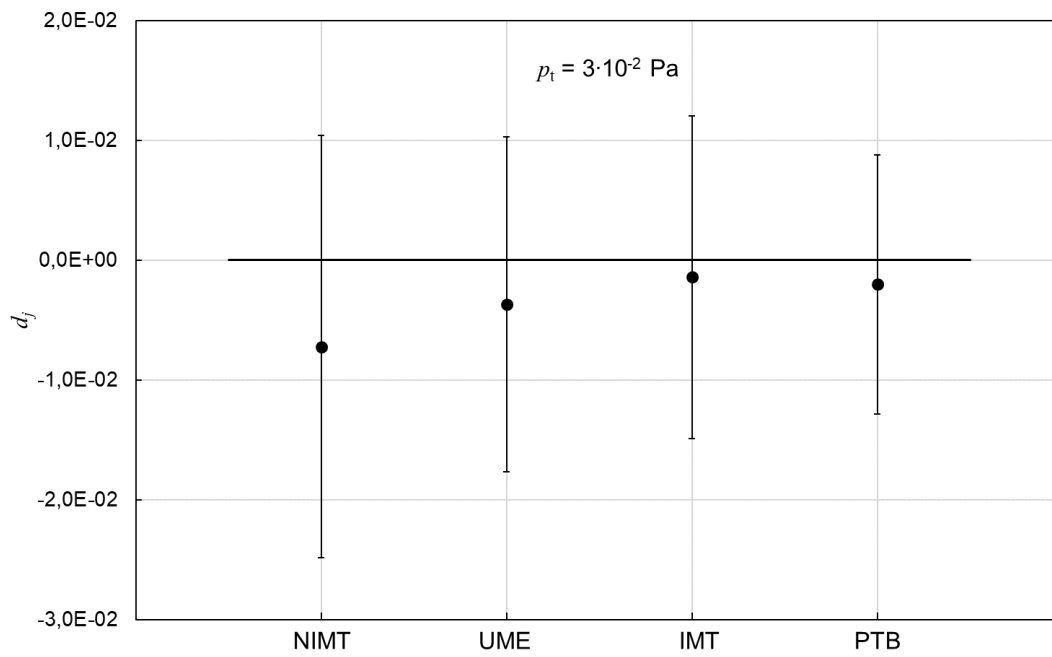
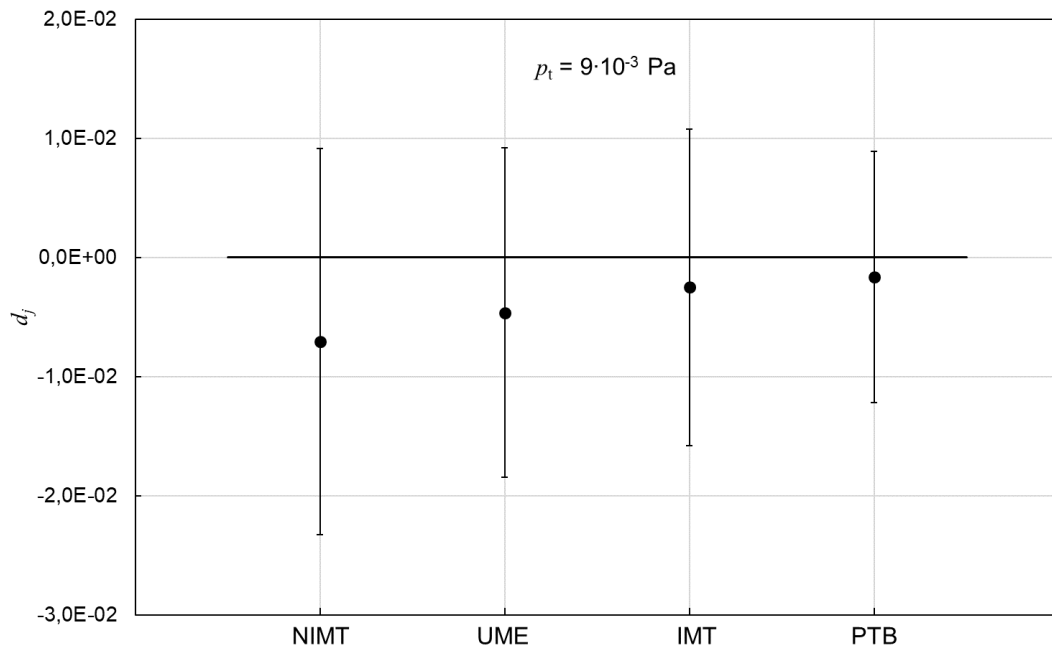
The values listed in Table 16 and

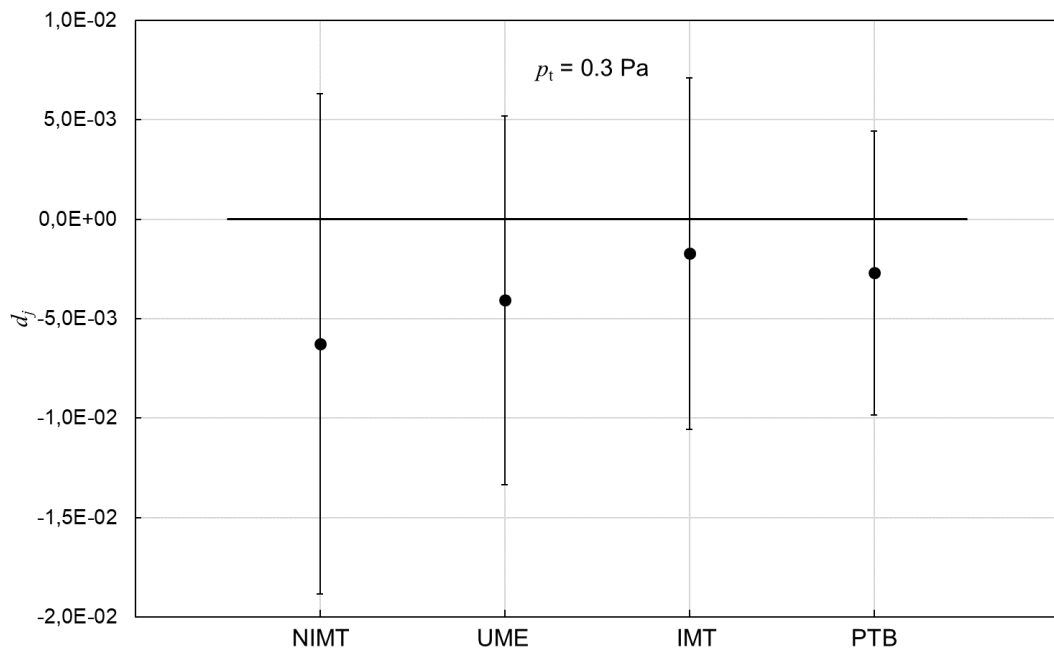
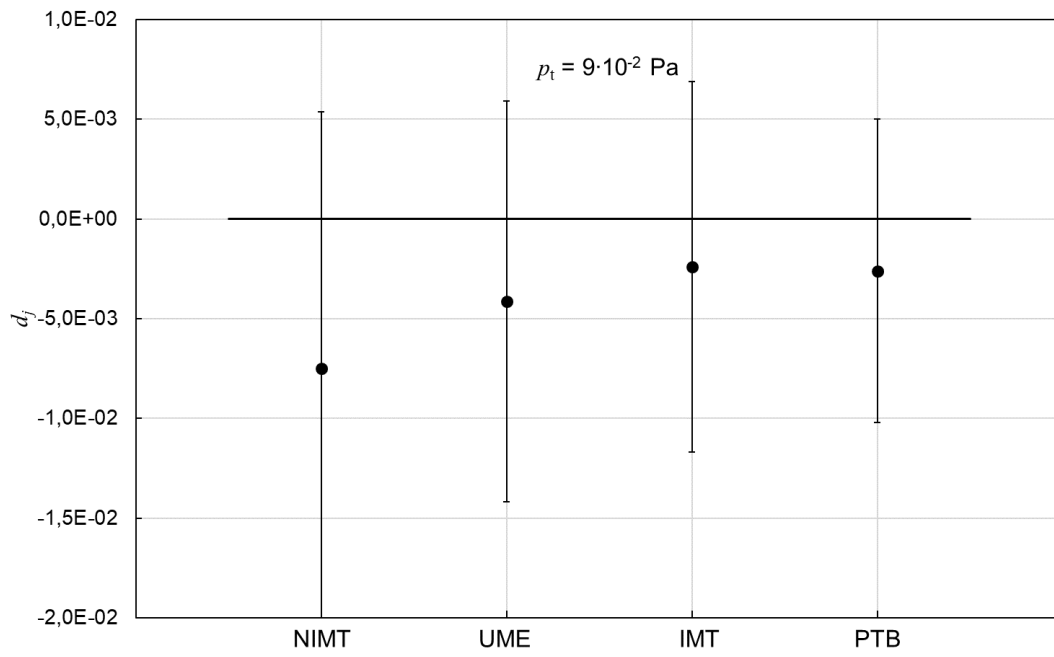
Table 17 are also shown target pressure wise in the Figure 5 and Figure 6.

Figure 5 Graphical illustration of the differences of predicted gauge readings of the participants and the predicted gauge readings, if PTB would have generated a pressure identical to the reference value of the comparison CCM.P-K15 (Eq. (26)). The expanded uncertainty is given by Eq. (27).









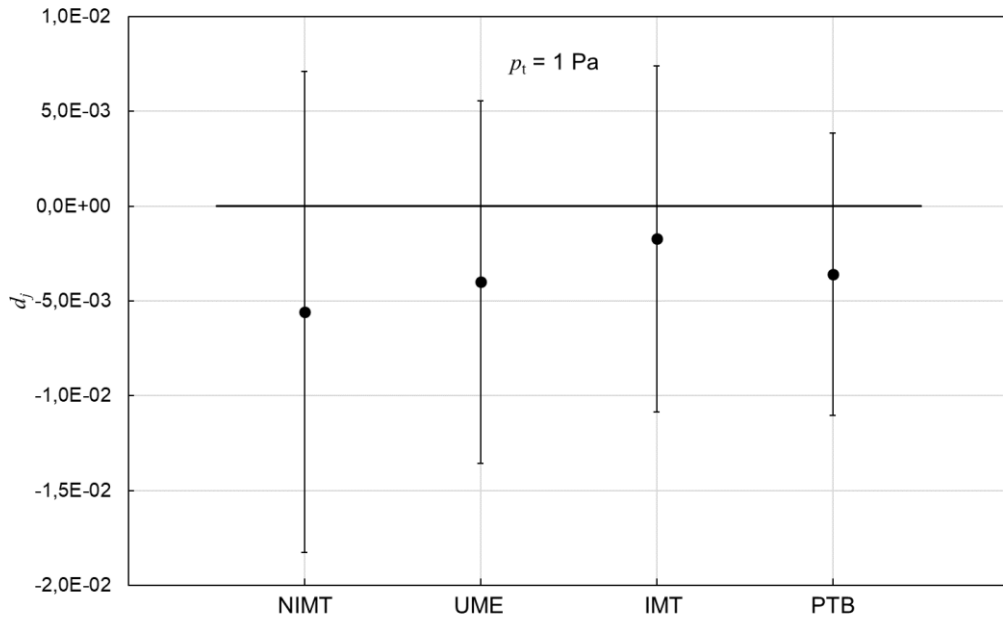
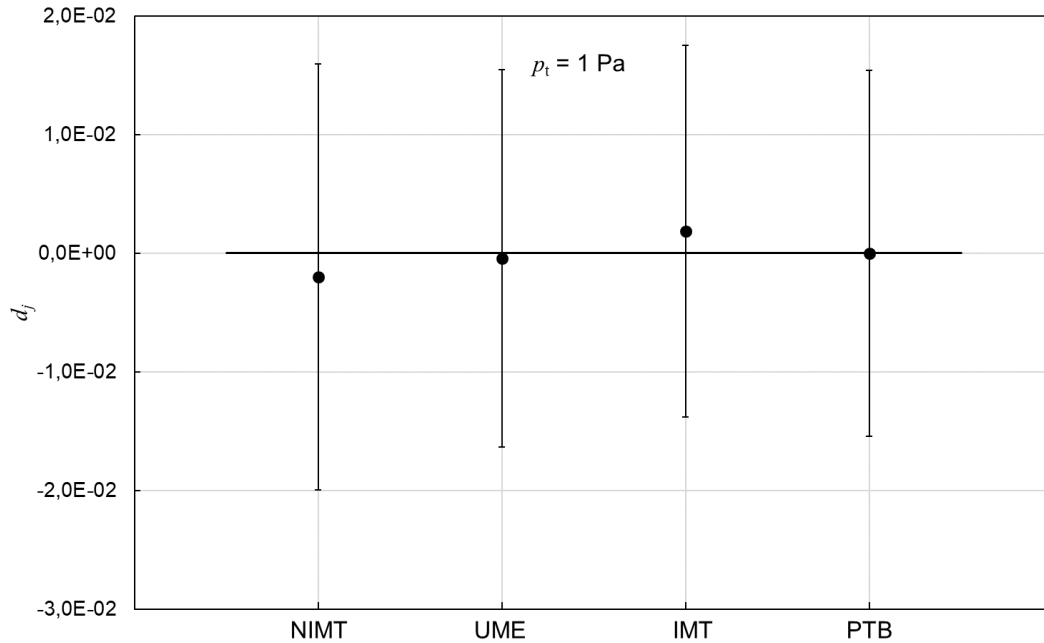


Figure 6 Graphical illustration of the differences of predicted gauge readings of the participants and the predicted gauge reading, if PTB would have generated a pressure identical to the reference value of the comparison CCM.P-K4 (Eq. (26)). The expanded uncertainty is given by Eq. (27).



12. Discussion and conclusions

In the present comparison, the degrees of equivalence of the measurement standards for vacuum pressures from $3 \cdot 10^{-4} \text{ Pa}$ up to 1 Pa of three NMIs were evaluated by comparison with the measurement standard of PTB serving as linking laboratory to the two comparisons CCM.P-K15 and CCM.P-K4. The

two SRGs used as transfer standards showed good transport stability, significantly better than the same type of transfer standards in CCM.P-K15 and Euromet.M.P-K1.b.

No common reference value of this comparison was determined, since with PTB there was only one linking laboratory. Instead, the predicted values of the transfer standards by PTB were calculated, as if PTB would have exactly generated the reference values of the mentioned key comparisons. These predicted values of the transfer standards served as reference for the predicted values of the other participants. The relative difference of the predicted gauge reading to the reference is to a very good approximation equal to the difference of generated or measured pressure in the standard to the reference, but of opposite sign.

All three NMIs and at all pressures showed equivalence with the key comparison reference values. For IMT and UME, equivalence was found for all pressures even on the $k=1$ level ($|E_n| \leq 0.5$). All absolute E_n values for NIMT were < 0.6 . There was a considerable difference between the two transfer standards for NIMT compared to the reference, but the mean of the two transfer standards was fully equivalent with the reference values. All E_n values of this comparison to the CCM.P-K15 reference value were negative. This may indicate that the reference value of CCM.P-K15 was too high. .

A fourth NMI, CEM, Spain, took part in the comparison, but did not deliver any data. Any consequences of this need to be discussed in the relevant Technical Committee of EURAMET and other committees involved.

13. References

- [1] Christian Wuethrich et al 2017 Metrologia 54 07003, <https://doi.org/10.1088/0026-1394/54/1A/07003>
- [2] Karl Jousten et al 2005 Metrologia 42 07001, <https://doi.org/10.1088/0026-1394/42/1A/07001>
- [3] K. Jousten, G. Rupschus, The uncertainties of calibration pressures at PTB, *Vacuum* **44** (1993), 569-572.
- [4] K. Jousten, P. Röhl, V. A. Contreras, Volume ratio determination in static expansion systems by means of a spinning rotor gauge, *Vacuum*, **52** (1999), 491...499.
- [5] W.Jitschin, J.K. Migwi, and G. Grosse, Pressures in the high and medium vacuum range generated by a series expansion standard, *Vacuum* 40 (1990), 293-304.
- [6] W.Jitschin, J.K. Migwi, and G. Grosse, Gauge calibration in the high and medium vacuum range by a series expansion standard, *Vacuum* 41 (1990), 1799.
- [7] Kangi R, Ongun B and Elkatmis A. Metrologia 2004; 41: 251-56
- [8] J. K. Fremerey, Spinning rotor gauges, *Vacuum* **32** (1982), 685...690.
- [9] S. Dittmann, B.E. Lindenau, C.R. Tilford, The molecular drag gauge as a calibration standard, *J. Vac. Sci. Technol. A* **7** (1989), 3356...3360.
- [10] J. A. Fedchak, K. Arai, K. Jousten, J. Setina, H. Yoshida, Recommended practices for the use of spinning rotor gauges in inter-laboratory comparisons, *Measurement* **66** (2015) 176–183.
- [11] P.Röhl and W. Jitschin, Performance of the SRG with a novel transport device as a transfer standard for high vacuum, *Vacuum* **38** (1988), 507...509.
- [12] K. Jousten, Is the effective accommodation factor of the spinning rotor gauge temperature dependent?, *J. Vac. Sci. Technol. A* **21**(1) (2003), 318...324.
- [13] R. Kacker and A. Jones, On use of Bayesian statistics to make the "Guide to the expression of uncertainty in measurement" consistent, *Metrologia* **40** (2003), 235 ... 248.
- [14] Chapter 15.2.4 in "Handbook of Vacuum Technology", 2nd edition, 2016, ed. Karl Jousten, WILEY-VCH, Weinheim, Germany.
- [15] Th. Bock, M. Bernien, Ch. Buchmann, T. Rubin, K. Jousten, Investigation of the effects of valve closing in a static expansion system, submitted to *Vacuum*, 2020

[16] J. Ricker et al., Final report on the key comparison CCM.P-K4.2012 in absolute pressure from 1 Pa to 10 kPa, Metrologia, Volume 54 (2017), Technical Supplement, 07002.